

Non-stochastic uncertainty response assessment method of beam and laminated plate using interval finite element analysis

Quoc Hoan Doan ^{1a}, Anh Tuan Luu ^{1b}, Dongkyu Lee ^{*1}, Jaehong Lee ^{1c} and Joowon Kang ^{2d}

¹ Department of Architectural Engineering, Sejong University, Seoul 05006, Republic of Korea

² Department of Architecture, Yeungnam University, Gyeongsan 38541, Republic of Korea

(Received December 20, 2019, Revised April 26, 2020, Accepted June 4, 2020)

Abstract. The goal of this study is to analytically and non-stochastically generate structural uncertainty behaviors of isotropic beams and laminated composite plates under plane stress conditions by using an interval finite element method. Uncertainty parameters of structural properties considering resistance and load effect are formulated by interval arithmetic and then linked to the finite element method. Under plane stress state, the isotropic cantilever beam is modeled and the laminated composite plate is cross-ply lay-up [0/90]. Triangular shape with a clamped-free boundary condition is given as geometry. Through uncertainties of both Young's modulus for resistance and applied forces for load effect, the change of structural maximum deflection and maximum von-Mises stress are analyzed. Numerical applications verify the effective generation of structural behavior uncertainties through the non-stochastic approach using interval arithmetic and immediately the feasibility of the present method.

Keywords: structural uncertainties; laminated composite plate; finite element method; interval arithmetic

1. Introduction

Beam and plate structures are frequently applied in many engineering applications such as buildings, bridges, aircraft, ships and so on. Therefore, an analytical or experimental process which investigates structural behaviors of the beam and plate is a significant task for engineers and designers (El-Shami *et al.* 2010, Xiao *et al.* 2016). Until now, a lot of studies (Awwad *et al.* 2014, Zirakian and Zhang 2015) were devoted to the industrial areas of beams and plates. Most of the features or characteristics of beams and plates have been well-known to engineers and designers. For example, loads applied to a beam may be a point load, uniformed or non-uniformed distributed loads, or varying loads. Besides, point moments or torsions may exist on the beam. The beam itself is supported at one or more points. Design conditions at the support depend on the kind of supports used. When the support is a roller, it can only have a reaction perpendicular to the motion of the roller. In a pinned support, it cannot carry a moment. When the support is fixed, then it can react in any direction and resist a moment as well. The beams can have various kinds of cross-sections, such as circular, elliptical, rectangular, I or L-shape, and so on. Comprehensive

knowledge of beam and plates could be found in the textbook of Timoshenko (1983) and Gere and Goodno (2013).

The excellent mechanical properties of composite materials (Leigh *et al.* 2012, Mahajan and Aher 2012, Liu *et al.* 2013, Manickam *et al.* 2015) such as high specific strength and stiffness, flexible anisotropic properties, ultra-lightweight and so on (Lee and Shin 2014, 2015) motivated researchers to study structural behaviors of laminated composite plates. A simple search of a popular website for the word "composite materials" yielded more than 250 entries. Many of these titles are published papers or excellent books on the mechanics of composite materials and have been adopted by educational institutions for introductory courses (Srinivas 1973, Hahn and Tsai 1980, Green and Naghdi 1982, Reddy 1994, 2004, Gibson 2011, Vinson and Sierakowski 2012).

Risk assessment (Tao *et al.* 2012, Stanley and John 2018, Zhang *et al.* 2019) is the determination of the quantitative or qualitative value of risk related to an obvious situation and a recognized threat, also called hazard. In all types of engineering of complex systems, sophisticated risk assessments are often made within safety engineering (Spellman and Whiting 2005, Lee *et al.* 2016, Nasr *et al.* 2018) and reliability engineering (Zio 2009, Zaitseva 2012, Abdulkadir and Altin 2014, Lee 2016, Sihombing and Torbol 2016), when it concerns threats to life, environment or machine functioning. The nuclear, aerospace, oil, rail and military industries have a long history of dealing with the risk assessment. Also, medical, hospital, social service, and food industries control the risks and perform the risk assessments continually. Methods for assessment of the risk

*Corresponding author, Associate Professor,

E-mail: dongkyulee@sejong.ac.kr

^a Ph.D. Student, E-mail: doanquochoan048@gmail.com

^b Ph.D. Student, E-mail: tuanla.hn@gmail.com

^c Professor

^d Professor

may differ between industries and whether it pertains to general financial decisions or environmental, ecological, or public health risk assessment.

One of the main problems in the structural assessment, especially, to beams and plates with composite materials is the treatment of uncertainty (Bulleit 2008, Aminifar and Marzuki 2013, Lee and Shin 2017) mainly presented in numerical models, physical and geometrical parameters such as applied loads, Young’s modulus, inertia, and so on, and in measured variables such as displacements, strains, and rotations. One of the main issues, while considering the various sources of uncertainty, is how to define objective and reliable criteria for distinguishing between an abnormal behavior (differences of measured values and those predicted by the model) due to the presence of damages, and the differences of measured and calculated results because of the uncertainty and randomness in the experimental data, models and physical parameters. When performing long term structural assessment, methodologies that take into account these uncertainties should be implemented in an efficient, fast and user-friendly way (García *et al.* 2008, Gazi and Alhan 2018, Ghiasia and Ghasemi 2018).

For the purpose, in this study, structural behaviors of the isotropic beam and laminated composite plates under plane stress conditions are analyzed with respect to structural uncertainty assessment. For the given representatives resulting in uncertainties of structural responses, applied load, and Young’s modulus is dealt with as uncertainty parameters. Uncertainty parameters are formulated by interval arithmetic describing the degree of uncertainty, which is linked to the initialization of finite element analysis. The variation of the deflection and von-Mises stress with respect to the uncertainty parameters are studied.

The content of this study is listed as follows. In Section 2, the finite element formulation of the composite plates under conditions of plane stress is presented. In Section 3, the uncertainty of Young’s modulus and applied force on the change of the structural maximum deflection and maximum von-Mises stress is described through interval arithmetic. In Section 4, the uncertainty analysis of the isotropic beams and laminated composite plates is presented under the conditions of geometrical triangular shape and clamped-free boundary conditions. The conclusions and remarks of this study are given in Section 5.

2. Formulations of finite element method for laminate plates

The resulting equation for the displacement-based finite element method is

$$[K]\{u\} = \{F\} \tag{1}$$

In the following, the stiffness matrix for laminated composite plates under plane stress conditions is generated. The general element stiffness matrix is derived for the plane stress problem in parametric space (ξ, η) as follow (Reddy 2006)

$$[K] = \begin{bmatrix} [K^{11}] & [K^2] \\ [K^1] & [K^2] \end{bmatrix} \tag{2}$$

where

$$K_{ij}^{11} = \int_{\Omega^e} \left[\left(A_{11} \frac{\partial \psi_i}{\partial \xi} \frac{\partial \psi_j}{\partial \xi} + A_{66} \frac{\partial \psi_i}{\partial \eta} \frac{\partial \psi_j}{\partial \eta} \right) + A_{16} \left(\frac{\partial \psi_i}{\partial \xi} \frac{\partial \psi_j}{\partial \eta} + \frac{\partial \psi_i}{\partial \eta} \frac{\partial \psi_j}{\partial \xi} \right) \right] d\xi d\eta \tag{3a}$$

$$K_{ij}^{12} = K_{ji}^{21} \int_{\Omega^e} \left(A_{16} \frac{\partial \psi_i}{\partial \xi} \frac{\partial \psi_j}{\partial \xi} + A_{26} \frac{\partial \psi_i}{\partial \eta} \frac{\partial \psi_j}{\partial \eta} + A_{12} \frac{\partial \psi_i}{\partial \xi} \frac{\partial \psi_j}{\partial \eta} + A_{66} \frac{\partial \psi_i}{\partial \eta} \frac{\partial \psi_j}{\partial \xi} \right) d\xi d\eta \tag{3b}$$

$$K_{ij}^{22} = \int_{\Omega^e} \left[\left(A_{66} \frac{\partial \psi_i}{\partial \xi} \frac{\partial \psi_j}{\partial \xi} + A_{22} \frac{\partial \psi_i}{\partial \eta} \frac{\partial \psi_j}{\partial \eta} \right) + A_{26} \left(\frac{\partial \psi_i}{\partial \xi} \frac{\partial \psi_j}{\partial \eta} + \frac{\partial \psi_i}{\partial \eta} \frac{\partial \psi_j}{\partial \xi} \right) \right] d\xi d\eta \tag{3c}$$

in which A_{ij} is the extensional stiffness which is defined in terms of the lamina stiffness $\bar{Q}_{ij}^{(k)}$ (Reddy 2004) as

$$A_{ij} = \sum_{k=1}^N \bar{Q}_{ij}^{(k)} (z_{k+1} - z_k) \tag{4}$$

where N is the number of lamina and details calculation of the lamina stiffness $\bar{Q}_{ij}^{(k)}$ could be found in the book by Reddy. And ψ_i are linear Lagrange interpolation functions and c_{ij} given for the constitutive equation as

$$\begin{Bmatrix} N_{xx} \\ N_{yy} \\ N_{xy} \end{Bmatrix} = \begin{bmatrix} A_{11} & A_{12} & A_{16} \\ A_{21} & A_{22} & A_{26} \\ A_{16} & A_{26} & A_{66} \end{bmatrix} \begin{Bmatrix} \varepsilon_{xx} \\ \varepsilon_{yy} \\ \gamma_{xy} \end{Bmatrix} \tag{5}$$

in which N_{xx} , N_{xy} , N_{yy} are the in-plane forces, ε_{xx} , ε_{yy} , γ_{xy} are in-plane strains. The parent element in parametric space is defined as shown in Fig. 1 and the linear Lagrange interpolation functions associated with rectangular elements can be obtained as

$$\psi_1 = \frac{1}{4}(1 - \xi)(1 - \eta) \tag{6a}$$

$$\psi_2 = \frac{1}{4}(1 + \xi)(1 - \eta) \tag{6b}$$

$$\psi_3 = \frac{1}{4}(1 + \xi)(1 + \eta) \tag{6c}$$

$$\psi_4 = \frac{1}{4}(1 - \xi)(1 + \eta) \tag{6d}$$

When the number of the lamina is one and the oriented direction is 0 degree, we have the orthotropic plate cases. And in the case of one lamina, $E_1 = E_2$, $G_{12} = \frac{E}{2(1+\nu)}$, we have the isotropic cases.

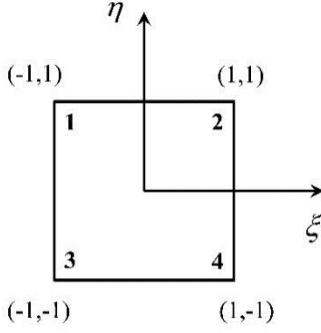


Fig. 1 Bi-linear parent element in parametric space

The displacements and von-Mises stress are calculated as

$$\{u\} = [K^{-1}]\{F\} \tag{7}$$

$$\sigma_{VM} = \sqrt{\sigma_1^2 + \sigma_2^2 - \sigma_1\sigma_2} \tag{8}$$

where σ_1 and σ_2 are principal stresses.

3. Formulations of structural parameters using interval arithmetic

3.1 Interval arithmetic considering uncertainties of structural parameters

Assume that $I(R)$, $I(R^n)$ and $I(R^{n \times n})$ denote the sets of all closed real interval numbers, n dimension real interval and n x n real interval matrices, respectively. R is the set of all real numbers, $X^I = [\underline{x}, \bar{x}]$ is a number of $I(R)$ and can be usually written in the following form

$$X^I = [X^C - \Delta X, X^C + \Delta X] \tag{9}$$

$$X^C = \frac{\underline{x} + \bar{x}}{2} \tag{10}$$

$$\Delta X = \frac{\bar{x} - \underline{x}}{2} \tag{11}$$

where X^C and ΔX denote the mean value of X^I and the uncertainty of X^I , respectively. The uncertain interval $\Delta X^I = [-\Delta X, \Delta X]$ indicates an interval change ratio with a given range of uncertainty.

An arbitrary interval $X^I = [\underline{x}, \bar{x}]$ can also be written as the sum of its mean value an uncertain interval: $X^I = X^C + \Delta X^I$.

3.2 Interval change function of Young's modulus E

It is assumed that E is not an exact value, and then the value of E exists within an interval with lower and upper bounds. $E = [\underline{E}, \bar{E}] = \{E \in R; \underline{E} \leq E \leq \bar{E}\}$ is the set of all real numbers are between infimum \underline{E} and the supremum \bar{E} .

The mean value of Young's modulus may be written as $E^C = \frac{\underline{E} + \bar{E}}{2}$, and the maximum width of Young's modulus is given as $\Delta E = \frac{\bar{E} - \underline{E}}{2}$.

Let f be a real-valued function of n real variables e_1, e_2, \dots, e_n . An extension of f means that an interval change function F of n interval variables E_1, E_2, \dots, E_n , for all $e_i \in E_i (i = 1, 2, \dots, n)$ possesses the following property $F([E_1, E_1], [E_2, E_2], \dots, [E_n, E_n]) = f(e_1, e_2, \dots, e_n)$.

The interval of E may also be expressed as

$$E = \left[E^C \left(1 - \frac{\Delta E}{E^C} \right), E^C \left(1 + \frac{\Delta E}{E^C} \right) \right] = \left[1 - \frac{\bar{E} - E}{2E^C}, 1 + \frac{\bar{E} - E}{2E^C} \right] E^C = E_F \cdot E^C \tag{12}$$

where interval change function of E is $E_F = \left[1 - \frac{\bar{E} - E}{2E^C}, 1 + \frac{\bar{E} - E}{2E^C} \right] = [E_F, \bar{E}_F]$ which $\underline{E}_F = 1 - \frac{\bar{E} - E}{2E^C}$ and $\bar{E}_F = 1 + \frac{\bar{E} - E}{2E^C}$.

Because E^C is the mean value of E and the uncertainty of E is denoted by E . Thus, E^F is called the interval factor of Young's modulus E .

The mean value of E_F is given by $E_F^C = \frac{\bar{E} + \underline{E}}{2} = 1$, and the maximum width of E_F is given by $\Delta E_F = \frac{\Delta E}{E^C}$.

ΔE_F can be considered as the interval change ratio value to assess the dispersal degree of the interval $[E, \bar{E}]$. Additionally, the interval factor of Young's modulus E can be written as the sum of its mean value and its uncertain interval ΔE_F with $\bar{E}_F = E_F^C + \Delta E_F = 1 + \frac{\Delta E}{E^C}$ and $E_F = E_F^C - \Delta E_F = 1 - \frac{\Delta E}{E^C}$.

3.3 Interval change function of applied load F

It is assumed that F is not an exact value, and then the value of F is changed in an interval. $F = [\underline{F}, \bar{F}] = \{F \in R; \underline{F} \leq F \leq \bar{F}\}$ is the set of all real numbers are between infimum \underline{F} and the supremum \bar{F} .

The mean value of the load is given by $F^C = \frac{\underline{F} + \bar{F}}{2}$ and the maximum width of the load is given by $\Delta F = \frac{\bar{F} - \underline{F}}{2}$.

Let f be a real-valued function of n real variables f_1, f_2, \dots, f_n . An extension of f means that an interval change function F of n interval variables F_1, F_2, \dots, F_n , for all $e_i \in F_i (i = 1, 2, \dots, n)$ possesses the following property $F([F_1, F_1], [F_2, F_2], \dots, [F_n, F_n]) = f(f_1, f_2, \dots, f_n)$.

The interval of load, F_I can also be expressed as

$$F_I = \left[F^C \left(1 - \frac{\Delta F}{F^C} \right), F^C \left(1 + \frac{\Delta F}{F^C} \right) \right] = \left[1 - \frac{\bar{F} - F}{2F^C}, 1 + \frac{\bar{F} - F}{2F^C} \right] F^C = F_F \cdot F^C \tag{13}$$

where interval change function of F is $F_F = \left[1 - \frac{\bar{F} - F}{2F^C}, 1 + \frac{\bar{F} - F}{2F^C} \right] = [F_F, \bar{F}_F]$ which $\underline{F}_F = 1 - \frac{\bar{F} - F}{2F^C}$ and $\bar{F}_F = 1 + \frac{\bar{F} - F}{2F^C}$.

Because F^C is the mean value of F and the uncertainty of F is denoted by F . Thus, F_F is called the interval factor of the load F .

The mean value of F_F is given by $F_F^C = \frac{\bar{F}+F}{2} = 1$ and the maximum width of E_F is given by $\Delta F_F = \frac{\Delta F}{F^C}$.

ΔF_F can be considered as the interval change ratio value to assess the dispersal degree of the interval $[\bar{F}, F]$. Additionally, the interval factor of the load F can be written as the sum of its mean value and its uncertain interval ΔF_F with $\bar{F}_F = F_F^C + \Delta F_F = 1 + \frac{\Delta F}{F^C}$ and $\underline{F}_F = F_F^C - \Delta F_F = 1 - \frac{\Delta F}{F^C}$.

In this study, interval change ratio is assumed to be a unit of given lower and upper bounds to show uncertainty ranges of uncertainty structural parameters such as values of Young's modulus and applied loads.

4. Numerical applications and discussion

To conduct survey in general, two kind of materials: homogeneous and non homogeneous with two representative structures are isotropic beam and composite plate are investigated in this part.

4.1 Isotropic cantilever beams

The cantilever beam with a triangular shape is modeled by 100×20 linear 4-node plane stress elements. The given interval change ratio is between 0 to 10% to describe the uncertainty degree of structural parameters. The schematic of the cantilever beam is depicted in Fig. 2, which denotes a real continuous model. Fig. 3 shows the discrete finite element model of the cantilever as shown in Fig. 2. Fig. 4 presents the von-Mises stress contour of the cantilever beam with Young's modulus $E = 1$, $\nu = 0.3$, and $F = -1$ as given nominal values. The effect of the uncertainty of Young's

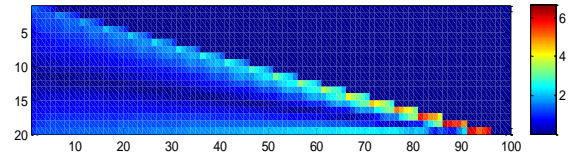


Fig. 4 von-Mises stress contour of the discrete modeled cantilever beam

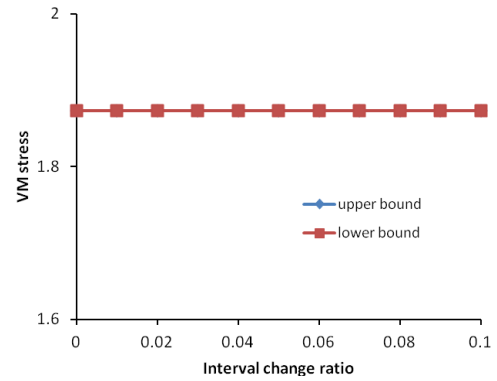


Fig. 5 von-Mises stress (ΔE)

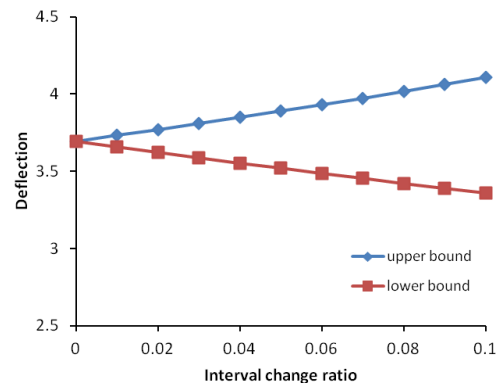


Fig. 6 Deflection (ΔE)

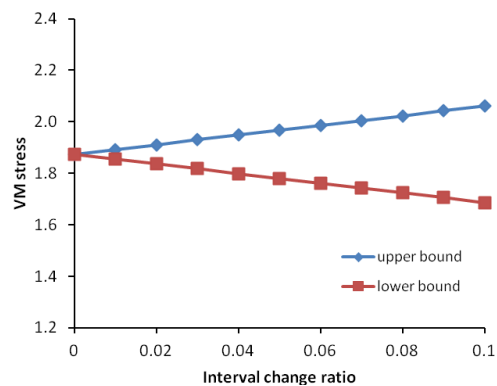


Fig. 7 von-Mises stress (ΔF)

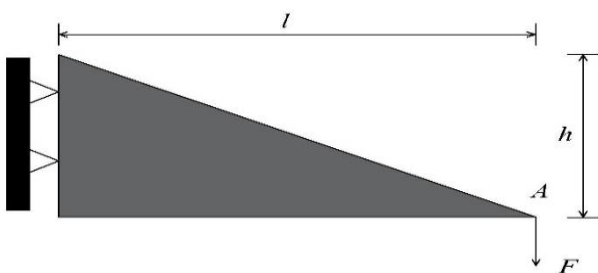


Fig. 2 Continuous real model of the cantilever beam with a triangular shape and a point load F

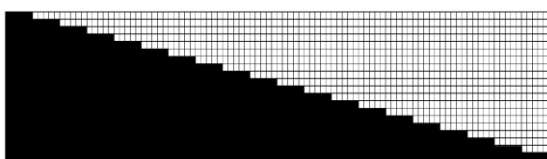


Fig. 3 Discrete finite element models for the cantilever: 100×20 4-node linear elements

modulus applied force on the change of the structural maximum deflection, and maximum von-Mises stress is described in Figs. 5 to 8. The uncertainty of them almost

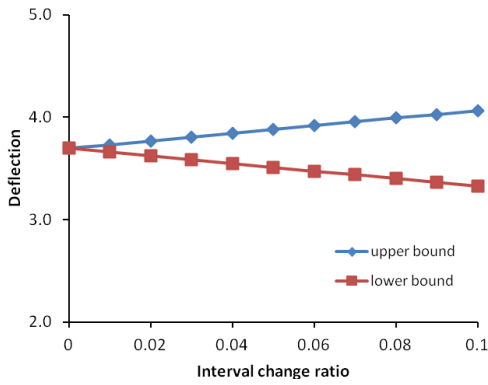


Fig. 8 Deflection (ΔF)

produces the same effect on structural deflection. Especially in Fig. 5, the von Mises stresses of the lower and upper bounds is totally same. It can be found that the uncertainty of Young’s modulus does not have any effect on the von-Mises stress.

Figs. 9 and 10 describe deflection curves at point A as shown in Fig. 2, according to the normalized applied load and Young’s modulus, respectively. As can be seen, the linear deflection curve for the normalized applied load is produced, but normalized Young’s modulus takes a nonlinear

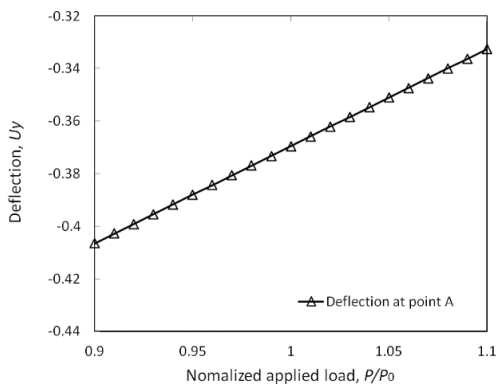


Fig. 9 Displacement at point A of the cantilever beam with respect to the normalized applied load

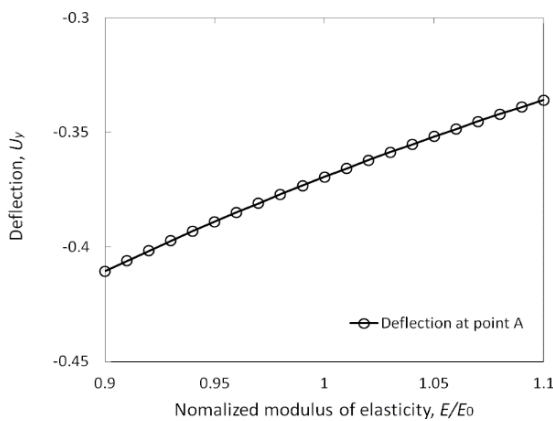


Fig. 10 Deflection at point A of the cantilever beam with respect to the normalized modulus of elasticity

deflection curve. This mean that the influence of applied load tends to increase linearly when the force is higher, but increase non-linearly in case of young modulus. In other words, the influence tended to decrease when the force is higher.

Moreover, it can be found that uncertainty behaviors of a material parameter such as Young’s modulus are reduced when uncertainty degree increases. Note that the present uncertainty behavior denotes structural behaviors resulting from uncertainty parameters. And uncertainty degree appeals to an uncertainty situation shown by interval change ratio.

4.2 Isotropic MBB beams

For the second application, the classical Messerschmitt-Bölkow-Blohm (MBB) beam is modeled for analysis which is a well-known simple supported beam in the structural optimization analysis. The schematic of MBB-beam with full design domain and half design domain with symmetric boundary conditions is depicted in Fig. 11.

The modulus of elasticity and point load is also uncertain parameters. MBB-beam is geometrically modeled like as the previous example but different boundary and loading conditions. That is, the finite element model is the same as in Fig. 2. von-Mises stress contour is shown in Fig. 12. The material properties are the same as the cantilever beam. The same procedure as the previous example is carried out for MBB-beam. Figs. 13 and 14 illustrate the variation of the deflection at point B with respect to the normalized applied load and normalized modulus of elasticity, respectively.

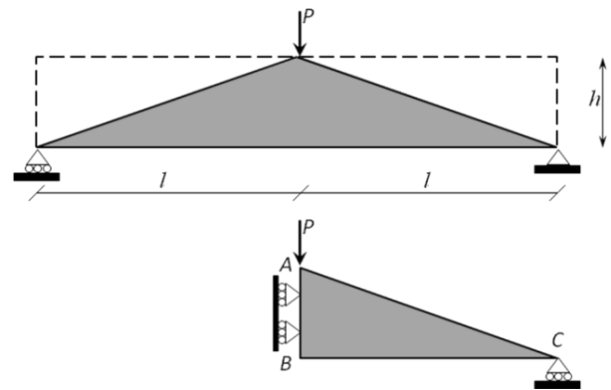


Fig. 11 Schematic of MBB-beam. Top: full design domain, and bottom: half design domain with symmetry boundary conditions

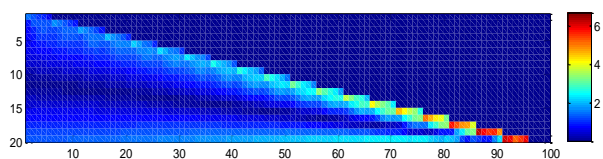


Fig. 12 Schematic of MBB-beam. Top: full design domain, and bottom: half design domain with symmetry boundary conditions

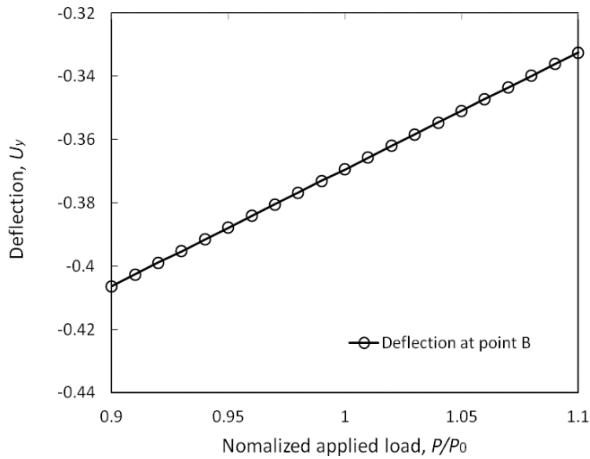


Fig. 13 Displacement at point B of the MBB-beam with respect to the normalized applied load

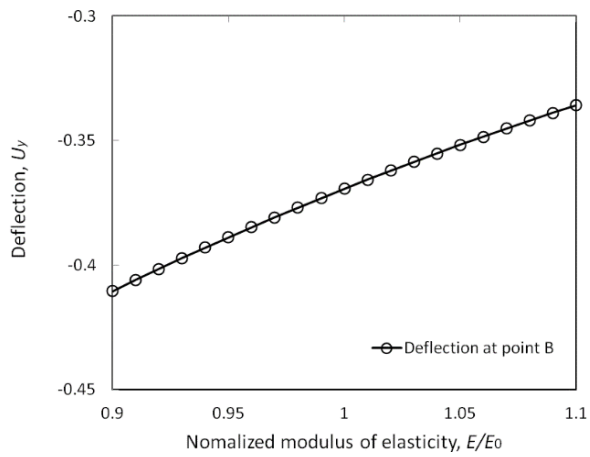


Fig. 14 Displacement at point B of the MBB-beam with respect to the normalized modulus of elasticity

As the same result of the previous application of the cantilever beam, uncertainty deflection behavior of material parameters such as Young’s modulus is gradually reduced when uncertainty degree increases.

4.3 Laminated composite plates

For the third application, the laminated composite plate is modeled for uncertainty interval analysis. The anti-symmetric cross-ply [0/90] lay-up is considered for the whole uncertainty analysis as shown in Fig. 15. The applied force and boundary conditions are the same as those of the cantilever beam as shown in Fig. 12. The plated is modeled by 40×40 linear 4-node elements for analyzing the uncertainty of Young’s modulus and applied force on the von-Mises stress. The following elastic properties are chosen for the composite material utilized in the laminate stacking sequences:

$E_1 = 15E_0$, $E_2 = E_0$, $G_{12} = 0.6E_0$, $\nu_{12} = 0.3$. Fig. 16(a) shows the finite element domain with 40×40 elements. Fig. 16(b) presents the von-Mises stress contour of the [0/90] cross-ply laminated plate with $E_0 = 10^3$, $P = -1$. The

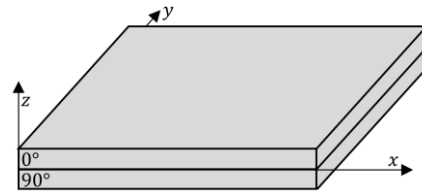


Fig. 15 Model of composite plates

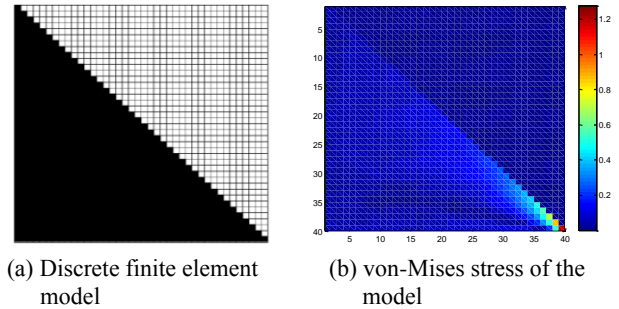


Fig. 16 Discrete finite element domain: 40×40 4-node linear elements and von-Mises stress contour

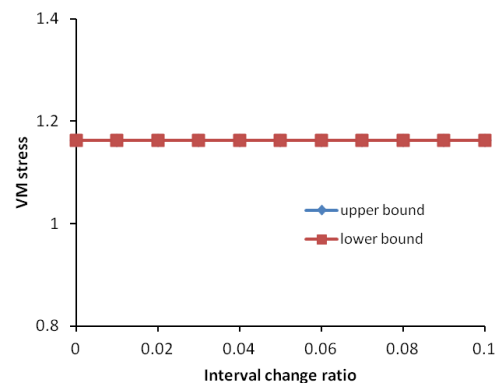


Fig. 17 von-Mises stress (ΔE_0)

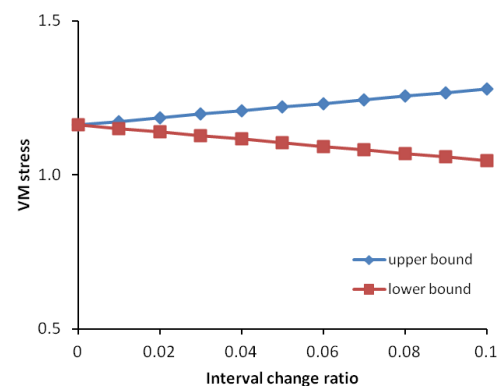


Fig. 18 von-Mises stress (ΔF)

Interval change ratio is given between 0 to 10%, and the value 0 means an assumption for conventional deterministic analysis.

The effect of the uncertainty of Young’s modulus applied force on the change of the maximum von-Mises

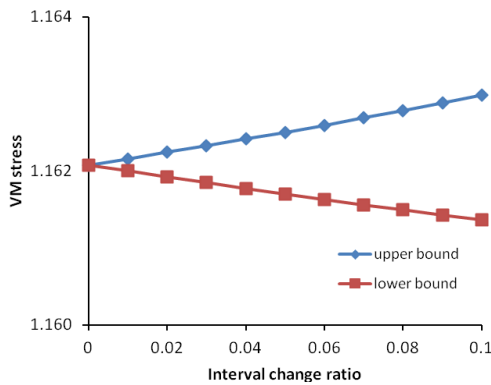


Fig. 19 von-Mises stress ($\Delta\lambda$)

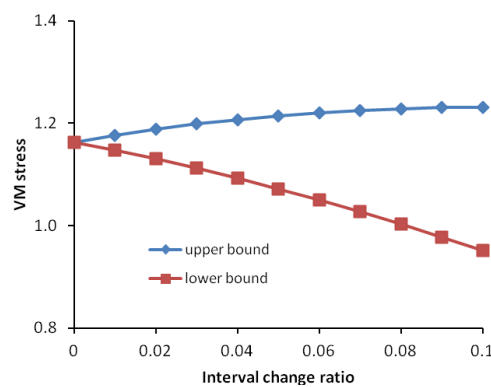


Fig. 20 von-Mises stress ($\Delta\alpha$)

stress is shown in Figs. 17 to 18. The uncertainty of the applied force F almost produces a significant effect on the von-Mises stress, however, the uncertainty of Young’s modulus does not have any effect on it.

The orthotropy ratio which is defined as $\lambda = E_1/E_2$ is considered for uncertainty interval analysis. The effect of uncertainty of the orthotropy ratio λ is shown in Fig. 19. The fiber change ratio is defined as $\alpha = \theta/\theta_0$ for the $[0/\theta]$ lay-up ($\theta_0 = 90^\circ$). The effect of uncertainty of the fiber change ratio on the change of maximum von-Mises stress is present in Fig. 20.

As can be seen in Figs. 19 and 20, von-Mises curve of lower and upper bounds of $\Delta\alpha$ tends to behave nonlinearly with respect to the interval change ratio. In the case of $\Delta\lambda$, von-Mises curves of lower and upper bounds produce almost linear curves.

5. Conclusions

In this research, the isotropic cantilever, MBB beam, and the $[0/90]$ cross-ply composite plate were analyzed for the uncertainty interval formulations of the deflection and von-Mises stress. The uncertainty behaviors produce linear or nonlinear curves of lower and upper bounds. The stiffness matrix is built for laminated composite plates under plane stress conditions. The isotropic cantilever beam is modeled by plane stress elements. From the presented results, the following concluding remarks are:

- There is no effect of the uncertainty of Young’s modulus on the von-Mises stress.
- The linear relationship is built between applied load and von-Mises stress as well as applied load and deflection.
- Non-linear relation is seen between Young’s modulus and deflection, and orthotropy ratio and von-Mises stress, and fiber angle change ratio and von-Mises stress.

Acknowledgments

This research was supported by a grant (NRF-2020R1A4A2002855) from NRF (National Research Foundation of Korea) funded by MEST (Ministry of Education and Science Technology) of Korean government.

References

Abdulkadir, T. and Altin, Z.G. (2014), “Statistical analysis of the effect of portland cement mortar’s performance containing glazed ceramic waste”, *J. Eng. Res.*, **2**(1), 133-146.

Aminifar, S. and Marzuki, A. (2013), “Uncertainty in Interval Type-2 Fuzzy Systems”, *Mathe. Probl. Eng.*, 2013.

Awwad, E., Hamad, B., Mabsout, M. and Khatib, H. (2014), *Structural Behavior of Simply Supported Beams Cast with Hemp-Reinforced Concrete*.

Bulleit, W.M. (2008), “Uncertainty in structural engineering”, *Practice Period. Struct. Des. Constr.*, **13**(1), 24-30. [https://doi.org/10.1061/\(ASCE\)1084-0680\(2008\)13:1\(24\)](https://doi.org/10.1061/(ASCE)1084-0680(2008)13:1(24))

El-Shami, M.M., Ibrahim, Y.E. and Shuaib, M. (2010), “Structural behavior of architectural glass plates”, *Alexandria Eng. J.*, **49**(4), 339-348. <https://doi.org/10.1016/j.aej.2010.07.001>

García, O., Vehí, J., Campos e Matos, J., Abel Henriques, A. and Ramon Casas, J. (2008), “Structural assessment under uncertain parameters via interval analysis”, *J. Computat. Appl. Mathe.*, **218**(1), 43-52. <https://doi.org/10.1016/j.cam.2007.04.047>

Gazi, H. and Alhan, C. (2018), “Probabilistic sensitivity of base-isolated buildings to uncertainties”, *Smart Struct. Syst., Int. J.*, **22**(4), 441-457. <https://doi.org/10.12989/sss.2018.22.4.441>

Gere, B.J. and Goodno, J.M. (2013), *Mechanics of Materials*, Cengage Learning, London, UK.

Ghiasia, R. and Ghasemi, M.R. (2018), “Optimization-based method for structural damage detection with consideration of uncertainties-a comparative study”, *Smart Struct. Syst., Int. J.*, **22**(5), 561-574. <https://doi.org/10.12989/sss.2018.22.5.561>

Gibson, R.F. (2011), *Principles of Composite Material Mechanics*, Third Edition, Taylor & Francis

Green, A.E. and Naghdi, P.M. (1982), “A theory of laminated composite plates”, *IMA J. Appl. Mathe.*, **29**(1), 1-23. <https://doi.org/10.1093/imamat/29.1.1>

Hahn, H.T. and Tsai, S.W. (1980), *Introduction to Composite Materials*, Taylor & Francis

Lee, D. (2016), *Additive 2D and 3D performance ratio analysis for steel outrigger alternative design*.

Lee, D. and Shin, S. (2014), “Advanced high strength steel tube diagrid using TRIZ and nonlinear pushover analysis”, *J. Constr. Steel Res.*, **96**, 151-158. <https://doi.org/10.1016/j.jcsr.2014.01.005>

Lee, D. and Shin, S. (2015), “High tensile UL700 frame module with adjustable control of length and angle”, *J. Constr. Steel Res.*, **106**, 246-257. <https://doi.org/10.1016/j.jcsr.2014.12.003>

Lee, D. and Shin, S. (2017), *Non-stochastic interval factor*

- method-based FEA for structural stress responses with uncertainty.
- Lee, D., Kim, Y., Shin, S. and Lee, J. (2016), "Real-time response assessment in steel frame remodeling using position-adjustment drift-curve formulations", *Automat. Constr.*, **62**, 57-65.
<https://doi.org/10.1016/j.autcon.2015.11.002>
- Leigh, S.J., Bradley, R.J., Pursell, C.P., Billson, D.R. and Hutchins, D.A. (2012), "A simple, low-cost conductive composite material for 3D printing of electronic sensors", *PLOS ONE*, **7**(11), e49365-e49365.
<https://doi.org/10.1371/journal.pone.0049365>
- Liu, W., Zhao, H., Yong, Z., Xu, G., Wang, X., Xu, F., Hui, D. and Qiu, Y. (2013), "Improving mechanical and electrical properties of oriented polymer-free multi-walled carbon nanotube paper by spraying while winding", *Compos. Part B: Eng.*, **53**, 342-346.
<https://doi.org/10.1016/j.compositesb.2013.05.043>
- Mahajan, G.V. and Aher, V.S. (2012), "Composite material: a review over current development and automotive application", *Int. J. Scientif. Res. Publicat.*, **2**(11), 1-5.
- Manickam, C., Kumar, J., Athijayamani, A. and Diwahar, N. (2015), "Mechanical and wear behaviors of untreated and alkali treated Roselle fiber-reinforced vinyl ester composite", *J. Eng. Res.*, **3**(3), 25-25. <https://doi.org/10.7603/s40632-015-0025-4>
- Nasr, D.E., Slika, W.G. and Saad, G.A. (2018), "Uncertainty quantification for structural health monitoring applications", *Smart Struct. Syst., Int. J.*, **22**(4), 399-411.
<https://doi.org/10.12989/sss.2018.22.4.399>
- Reddy, J.N.E. (1994), *Mechanics of Composite Materials - Selected Works of Nicholas J. Pagano*, Springer Netherlands
- Reddy, J.N. (2004), *Mechanics of Laminated Composite Plates and Shells: Theory and Analysis*, Second Edition, CRC Press
- Reddy, J.N. (2006), *Introduction to the Finite Element Method*, Third Edition, McGraw-Hill Education, New York.
- Sihombing, F. and Torbol, M. (2016), "Analytical fragility curves of a structure subject to tsunami waves using smooth particle hydrodynamics", *Smart Struct. Syst., Int. J.*, **18**(6), 1145-1167.
<https://doi.org/10.12989/sss.2016.18.6.1145>
- Spellman, F.R. and Whiting, N.E. (2005), *Safety Engineering: Principles and Practices*, Government Institutes
- Srinivas, S. (1973), "A refined analysis of composite laminates", *J. Sound Vib.*, **30**(4), 495-507.
- Stanley, K. and John, G.B. (2018), "On the quantitative definition of risk", *Risk Anal.*, **1**(1), 11-27.
<https://doi.org/10.1111/j.1539-6924.1981.tb01350.x>
- Tao, Z., Huajun, L. and Defu, L. (2012), "Risk assessment method for offshore structure based on global sensitivity analysis", *Model. Simul. Eng.*, 2012.
<https://doi.org/10.1155/2012/671934>
- Timoshenko, S. (1983), *Strength of Materials*, Pt. 2: Advanced Theory and Problems, Krieger Publishing Company
- Vinson, J.R. and Sierakowski, R.L. (2012), *The behavior of structures composed of composite materials*, Springer Netherlands.
- Xiao, G., Qingsong, L., Daxu, Z. and Jinghai, G. (2016), "Structural behavior of an air-inflated fabric arch frame", *J. Struct. Eng.*, **142**(2), 4015108-4015108.
[https://doi.org/10.1061/\(ASCE\)ST.1943-541X.0001374](https://doi.org/10.1061/(ASCE)ST.1943-541X.0001374)
- Zaitseva, E. (2012), *Importance Measures in Reliability Analysis of Healthcare System BT - Human - Computer Systems Interaction: Backgrounds and Applications 2: Part 1*, Springer Berlin Heidelberg, Berlin, Heidelberg.
- Zhang, Q., Tang, X., Wu, J. and Yang, B. (2019), "Online automatic structural health assessment of the Shanghai Tower", *Smart Struct. Syst., Int. J.*, **24**(3), 319-332.
<https://doi.org/10.12989/sss.2019.24.3.319>
- Zio, E. (2009), "Reliability engineering: Old problems and new challenges", *Reliabil. Eng. Syst. Safe.*, **94**(2), 125-141.
<https://doi.org/10.1016/j.res.2008.06.002>
- Zirakian, T. and Zhang, J. (2015), "Seismic design and behavior of low yield point steel plate shear walls", *Int. J. Steel Struct.*, **15**(1), 135-151. <https://doi.org/10.1007/s13296-015-3010-8>

CC